Inorganic Chemistry

ARTICLE

pubs.acs.org/IC

Synthesis, Antimicrobial and Antiproliferative Activity of Novel Silver(I) Tris(pyrazolyl)methanesulfonate and 1,3,5-Triaza-7-phosphadamantane Complexes

Claudio Pettinari,[*,†] Fabio Marchetti,[‡] Giulio Lupidi,[†] Luana Quassinti,[†] Massimo Bramucci,[†] Dezemona Petrelli,[†] Luca A. Vitali,[†] M. Fátima C. Guedes da Silva,[*,§,⊥] Luísa M. D. R. S. Martins,[§,∥] Piotr Smoleński,[*,⊗] and Armando J. L. Pombeiro[*,§]

[†]School of Pharmacy and [‡]School of Science and Technology, Università degli Studi di Camerino, via S Agostino 1, 62032 Camerino MC, Italy

[§]Centro de Química Estrutural, Complexo I, Instituto Superior Técnico, Technical University of Lisbon, Av. Rovisco Pais, 1049-001 Lisbon, Portugal

[⊥]Universidade Lusófona de Humanidades e Tecnologias, ULHT Lisbon, Campo Grande 376, 1749-024 Lisboa, Portugal

[∥]Área Departamental de Engenharia Química, Instituto Superior de Engenharia de Lisboa, Rua Conselheiro Emídio Navarro, 1059-007, Lisboa, Portugal

[⊗]Faculty of Chemistry, University of Wroclaw, ul. F. Joliot-Curie 14,50-383 Wroclaw, Poland

Supporting Information

ABSTRACT: Five new silver(I) complexes of formulas [Ag(Tpms)] (**1**), [Ag(Tpms)(PPh$_3$)] (**2**), [Ag(Tpms)(PCy$_3$)] (**3**), [Ag(PTA)][BF$_4$] (**4**), and [Ag(Tpms)(PTA)] (**5**) {Tpms = tris(pyrazol-1-yl)methanesulfonate, PPh$_3$ = triphenylphosphane, PCy$_3$ = tricyclohexylphosphane, PTA = 1,3,5-triaza-7-phosphaadamantane} have been synthesized and fully characterized by elemental analyses, ^{1}H, ^{13}C, and ^{31}P NMR, electrospray ionization mass spectrometry (ESI-MS), and IR spectroscopic techniques. The single crystal X-ray diffraction study of **3** shows the Tpms ligand acting in the N$_3$-facially coordinating mode, while in **2** and **5** a N$_2$O-coordination is found, with the SO$_3$ group bonded to silver and a pendant free pyrazolyl ring. Features of the tilting in the coordinated pyrazolyl rings in these cases suggest that this inequivalence is related with the cone angles of the phosphanes. A detailed study of antimycobacterial and antiproliferative properties of all compounds has been carried out. They were screened for their in vitro antimicrobial activities against the standard strains *Enterococcus faecalis* (ATCC 29922), *Staphylococcus aureus* (ATCC 25923), *Streptococcus pneumoniae* (ATCC 49619), *Streptococcus pyogenes* (SF37), *Streptococcus sanguinis* (SK36), *Streptococcus mutans* (UA159), *Escherichia coli* (ATCC 25922), and the fungus *Candida albicans* (ATCC 24443). Complexes **1**−**5** have been found to display effective antimicrobial activity against the series of bacteria and fungi, and some of them are potential candidates for antiseptic or disinfectant drugs. Interaction of Ag complexes with deoxyribonucleic acid (DNA) has been studied by fluorescence spectroscopic techniques, using ethidium bromide (EB) as a fluorescence probe of DNA. The decrease in the fluorescence of DNA−EB system on addition of Ag complexes shows that the fluorescence quenching of DNA−EB complex occurs and compound **3** is particularly active. Complexes **1**−**5** exhibit pronounced antiproliferative activity against human malignant melanoma (A375) with an activity often higher than that of AgNO$_3$, which has been used as a control, following the same order of activity inhibition on DNA, i.e., **3** > **2** > **1** > **5** > **AgNO$_3$** ≫ **4**.

INTRODUCTION

Biomedical inorganic chemistry is an important new area of chemistry that plays a significant role in therapeutic and diagnostic medicine for the discovery and development of new metallodrugs.[1] Among the metal complexes used for treatment of several diseases,[2] some silver complexes are currently applied as antibacterial agents in therapeutic protocols.[3,4] In view of their potent antimicrobial properties and low human toxicity, metallic silver or silver complexes have been used in a variety of applications such as water purification, wound management, eye-drops, anti-infective coatings in medical devices (e.g., in dental work or catheters), and healing of burn wounds.[5−12] They were shown to have a pleiotropic effect on the bacterial cell and most probably interact with proteins involved in maintaining the proton motive force through the cytoplasmic membrane or in the respiration of the bacteria,[13,14] although other target sites remain a possibility.[15] The interaction of silver ions with thiol groups in enzymes and

Received: August 6, 2011
Published: October 14, 2011

dx.doi.org/10.1021/ic201714c | *Inorg. Chem.* 2011, 50, 11173–11183

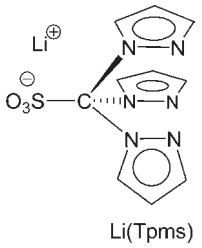

Li(Tpms)

Figure 1. Lithium derivative of Tpms ligand.

proteins plays an essential role in its antimicrobial action, although other cellular contributions, like hydrogen bonding, may also be involved. In addition to their effects on bacterial enzymes, silver ions cause marked inhibition of bacterial growth. They deposit in the vacuole and cell wall as granules, inhibit cell division and damage the cell envelope and contents of bacteria.[16] Bacterial cells increase in size, and the cytoplasmic membrane, cytoplasmic contents, and outer cell layers exhibit structural abnormalities. An interaction of silver ions with the bases of nucleic acids has been also described,[17] although the implication of this in terms of their bactericidal activity is still questioned.

Many silver complexes are sparingly soluble in common solvents, especially water, which limits their uses in oil treatments and creams, as for the most used topical antibacterial agent silversulfadiazine (SSD).[18] Moreover, since antimicrobial resistance is growing at a frightening rate (microorganisms such as methicillin-resistant *Staphylococcus aureus*, staphylococci with decreased susceptibility to vancomycin, vancomycin-resistant enterococci, multidrug resistant Gram-negatives, as well as *Streptococcus pneumoniae* with decreased susceptibility to penicillin and other antibacterials are frequently isolated in both hospital and community settings), there is a growing need for novel agents or an improvement of the existing ones to combat resistant organisms.

Silver complexes are also particularly interesting since the antimicrobial activity and other desirable properties can be tuned by varying the number and type of ligands. For example, the silver(I) imidazolate complex has excellent antibacterial and antifungal properties,[19] while its PPh_3 adduct essentially does not show antimicrobial activity.[20] Silver(I) sulfadiazine, a polymeric complex releasing silver ions slowly, is one of the most popular silver based antimicrobial agents for treating infections on severe burn sites.[11,12,21−24]

Following a recent series of studies[25−28] on complexes formed upon reactions of silver(I) oxyanions salts with (mostly) uni- and bidentate ligands based on pyridine and azoles, we now report the synthesis and bioactivity of new silver(I) derivatives with a different type of ligand, of the family of anionic scorpionates, that is, tris(pyrazol-1-yl)methanesulfonate (Tpms). This has recently been shown to possess interesting structural and electronic features with respect to classical tris(pyrazol-1-yl)borate (Tp).[29,30] Tpms (Figure 1) bears a methanesulfonate group at the place of the B−H moiety in Tp, which confers good stability toward hydrolysis and increased solubility in polar solvents, such as water or methanol.

Tpms and analogous species having different substituents in the 3-position of the pyrazole rings exhibit a marked coordination versatility, acting either as a tripodal or a bipodal ligand (i.e., with N_3-, N_2O-, N_2-, or NO- coordination modes) with the possibility of involving the sulfonate moiety in the coordination, hence being suitable ligands for the synthesis of structural models for *N,N,O*-binding in metalloenzymes.[30a] The new silver complexes here reported were obtained from reaction of $AgBF_4$ with Tpms, also in the presence of some monodentate phosphanes (triphenylphosphane, PPh_3, tricyclohexylphosphane, PCy_3, and the water-soluble 1,3,5-triaza-7-phosphaadamantane, PTA).[30] Their antimicrobial activity is also reported. In addition, since the anticancer activity of silver complexes was recently demonstrated,[31−34] we have also investigated their antiproliferative activity against human malignant melanoma cells.

EXPERIMENTAL SECTION

Materials and Physical Measurements. All chemicals were purchased from Aldrich (Milwaukee) and used as received. Lithium derivative of the scorpionate Tpms ligand was synthesized as previously reported.[29a] All of the reactions and manipulations were performed in the air. Solvent evaporations were always carried out under vacuum conditions using a rotary evaporator. The samples for microanalyses were dried in vacuo to constant weight (20 °C, ca. 0.1 Torr). Elemental analyses (C, H, N, S) were performed in-house with a Fisons Instruments 1108 CHNS-O Elemental Analyzer. IR spectra were recorded from 4000 to 400 cm^{-1} with a Perkin-Elmer Spectrum 100 FT-IR instrument. ^1H, $^{31}P\{^1H\}$, and $^{13}C\{^1H\}$ NMR spectra were recorded on a 400 Mercury Plus Varian instrument operating at room temperature (400 MHz for ^1H, 162.1 MHz for ^{31}P, and 100 MHz for ^{13}C). H and C chemical shifts (δ) are reported in parts per million (ppm) from $SiMe_4$ (^1H and ^{13}C calibration by internal deuterium solvent lock) while P chemical shifts (δ) are reported in ppm versus 85% H_3PO_4. Melting points are uncorrected and were taken on an STMP3 Stuart scientific instrument and on a capillary apparatus. The electrical conductivity measurements (Λ_M, reported as S cm^2 mol^{-1}) of dimethylsulfoxide (DMSO), acetone, and water solutions of the silver derivatives were taken with a Crison CDTM 522 conductimeter at room temperature (r.t.). The positive and negative electrospray mass spectra were obtained with a Series 1100 MSI detector HP spectrometer, using an acetonitrile mobile phase. Solutions (3 mg/mL) for electrospray ionization mass spectrometry (ESI-MS) were prepared using reagent-grade acetonitrile. For the ESI-MS data, mass and intensities were compared to those calculated using IsoPro Isotopic Abundance Simulator, version 3.1.[35] Peaks containing silver(I) ions were identified as the center of an isotopic cluster.

Synthesis of the Silver Compounds 1−5. *[Ag(Tpms)] (**1**).* A solution of Li(Tpms) (0.077 g, 0.26 mmol) in methanol (10 mL) was added dropwise to a solution of $AgBF_4$ (0.050 g, 0.26 mmol) in methanol (10 mL). After 6 h stirring at r.t., the suspension was filtered off, and the grayish-rose precipitate of **1** was dried under reduced pressure. **1** is soluble in DMSO and poorly soluble in acetonitrile. Yield 0.083 g, 80%. *Mp* 310 °C (dec). Anal. Calcd. for $C_{10}H_9AgN_6O_3S$: C, 29.94; H, 2.26; N, 20.95; S, 7.99. Found: C, 29.65; H, 2.29; N, 20.64; S, 7.71%. Λ_M (DMSO, 298 K, 10^{-3} mol/L) 1.3 S cm^2 mol^{-1}. IR (KBr, cm^{-1}): 3145w, 3133w, 3108w $\nu(C_{arom}-H)$, 1522 m $\nu(C{=}N)$, 1427 m, 1396 m, 1325 m, 1268vs, 1259s, 1214w, 1199w, 1104 m, 1097 m, 1061 m, 1056 m, 1046s $\nu(SO_3)$, 1104s, 1096 ν(ring), 866 m, 857s, 847s $\nu(C-N)$, 635s $\nu(C-S)$. ^1H NMR (CD_3CN, 298 K): δ, 6.40dd (3H, 4-H (pz)), 7.54d (3H, 3,5-H (pz)), 8.20d (3H, 3,5-H (pz)). ^1H NMR (DMSO-d_6, 298 K): δ, 6.36dd (3H, 4-H (pz)), 7.46d (3H, 3,5-H (pz)), 8.11d (3H, 3,5-H (pz)). ^{13}C NMR (DMSO-d_6, 298 K): δ, 95.41s (CSO_3) 106.53s ($C4_{pz}$), 132.84s ($C5_{pz}$), 140.34s ($C3_{pz}$). ESI^+-MS (CH_3CN) m/z: 149 $[Ag(CH_3CN)]^+$, 190 $[Ag(CH_3CN)_2]^+$, 550 $[Ag_2(Tpms)(CH_3CN)]^+$, 591 $[Ag_2(Tpms)(CH_3CN)_2]^+$. ESI^--MS (CH_3CN) m/z: = 293 $[Tpms]^-$, 694 $[Ag(Tpms)_2]^-$, 1096 $[(Ag)_2(Tpms)_3]^-$.

dx.doi.org/10.1021/ic201714c |*Inorg. Chem.* 2011, 50, 11173–11183

[Ag(Tpms)(PPh$_3$)] (**2**). $AgBF_4$ (0.050 g, 0.26 mmol) was dissolved in methanol (20 mL) and the solution stirred for 30 min, then PPh_3 (0.067 g, 0.26 mmol) and Li(Tpms) (0.077 g, 0.26 mmol) were added. After 24 h stirring at r.t. the precipitate was removed by filtration. The solution was evaporated to dryness, and the solid dissolved in diethyl ether (5 mL). Slow evaporation afforded a pale-rose powder of **2**, which was dried under reduced pressure. **2** is very soluble in alcohols, chlorinated solvents, acetonitrile, acetone, and DMSO. Yield 0.103 g, 60%. *Mp* 185−186 °C. Anal. Calcd. for $C_{28}H_{24}AgN_6O_3PS$: C, 50.69; H, 3.65; N, 12.67; S, 4.83. Found: C, 50.21; H, 3.67; N, 12.33; S, 4.32%. Λ_M (CH_3CN, 298 K, 10^{-3} mol/L) 4.7 S cm^2 mol^{-1}. IR (KBr, cm^{-1}): 3156w, 3114w, 3125w, 3056w ν(C$_{arom}$−H), 1522 m ν(C═N), 1480 m, 1435 m, 1414 m, 1381 m, 1330 m, 1313 m, 1272s, 1260vs, 1245vs, 1200 m, 1051vs, 1041s ν(SO_3), 1096vs ν(ring), 857 m, 846 m ν(C−N), 628s ν(C−S), 524s, 505s ν(PPh_3). ^{1}H NMR ($CDCl_3$, 298 K): δ, 6.38dd (3H, 4-H (pz)), 7.25−7.45 m br (15H, P−C$_6H_5$), 7.62d (3H, 3,5-H (pz)), 7.98d (3H, 3,5-H (pz)). ^{1}H NMR ($CDCl_3$, 253 K): δ, 6.36dd (3H, 4-H (pz)), 7.26−7.52 m br (15H, P−C$_6H_5$), 7.74d (3H, 3,5-H (pz)), 8.01d (3H, 3,5-H (pz)). ^{1}H NMR ($CDCl_3$, 223 K): δ, 6.37br (3H, 4-H (pz)), 7.30−7.55 m br (15H, P−C$_6H_5$), 7.75br (3H, 3,5-H (pz)), 8.01br (3H, 3,5-H (pz)). ^{1}H NMR (CD_3OD, 298 K): δ, 6.47dd (3H, 4-H (pz)), 7.44−7.52 m br (15H, P−C$_6H_5$), 7.66d (3H, 3,5-H (pz)), 8.08d (3H, 3,5-H (pz)). ^{1}H NMR (acetone-d_6, 298 K): δ, 6.46t (3H, 4-H (pz)), 7.50−7.65 m br (15H, P−C$_6H_5$), 7.75d (3H, 3,5-H (pz)), 8.24d (3H, 3,5-H (pz)). ^{1}H NMR (acetone-d_6, 203 K): δ, 6.46br (3H, 4-H (pz)), 7.40−7.50 m br, 7.60−7.65 m br (15H, P−C$_6H_5$), 7.95br (3H, 3,5-H (pz)), 8.22br (3H, 3,5-H (pz)). ^{1}H NMR (acetone-d_6, 183 K): δ, 6.45br, 6.60br (3H, 4-H (pz)), 7.40−7.50 m br, 7.60−7.65 m br (15H, P−C$_6H_5$), 8.00br, 8.22br (3H, 3,5-H (pz)), 8.50br, 8.59br (3H, 3,5-H (pz)). ^{13}C NMR (acetone-d_6, 298 K): δ, 107.6s (C4$_{pz}$), 130.3d (C$_{arom}$, 11.0 Hz), 132.0d (C$_{arom}$, 1.6 Hz), 132.2d br (C$_{ipso}$) 134.7d (C$_{arom}$, 17.0 Hz) 135.2 (C5$_{pz}$), 143.1s (C3$_{pz}$). ^{31}P{^{1}H} NMR ($CDCl_3$, 298 K): δ, 16.5dbr (^1J(^{31}P-$^{109/107}$Ag): 696 Hz). ^{31}P{^{1}H}NMR (acetone-d_6, 298 K): δ, 16.9dbr (^1J(^{31}P-$^{109/107}$Ag): 688 Hz). ^{31}P{^{1}H} NMR (acetone-d_6, 263 K): δ, 16.4dd (^1J(^{31}P-^{109}Ag): 775 Hz; ^1J(^{31}P-^{107}Ag): 674 Hz). ^{31}P{^{1}H} NMR (acetone-d$_6$, 233 K): δ, 15.9dd (^1J(^{31}P-^{109}Ag): 776 Hz; ^1J(^{31}P-^{107}Ag): 672 Hz). ^{31}P{^{1}H} NMR (acetone-d_6, 203 K): δ, 15.4ddbr (^1J(^{31}P-^{109}Ag): 737 Hz; ^1J(^{31}P-^{107}Ag): 638 Hz). ^{31}P{^{1}H} NMR (acetone-d_6, 183 K): δ, 15.8ddbr (^1J(^{31}P-^{109}Ag): 745 Hz; ^1J(^{31}P-^{107}Ag): 650 Hz), 15.1ddbr (^1J(^{31}P-^{109}Ag): 786 Hz; ^1J(^{31}P-^{107}Ag): 686 Hz), 13.1ddbr (^1J(^{31}P-^{109}Ag): 713 Hz; ^1J(^{31}P-^{107}Ag): 616 Hz). ESI$^+$-MS (CH_3OH) *m*/*z*: 632 [Ag(PPh_3)$_2$]$^+$, 686 [Ag(Tpms)(PPh_3)Na]$^+$, 1034 [(Ag)$_2$(Tpms)(PPh_3)$_2$]$^+$.

[Ag(Tpms)(PCy$_3$)] (**3**). $AgBF_4$ (0.050 g, 0.26 mmol) was dissolved in methanol (20 mL) and stirred for 30 min, then PCy_3 (0.072 g, 0.26 mmol) and Li(Tpms) (0.077 g, 0.26 mmol) were added. After 24 h stirring at r.t. the precipitate ($LiBF_4$) was removed by filtration. Slow evaporation of the solution afforded a brown crystalline solid of **3** which was dried under reduced pressure. Compound **3** is very soluble in alcohols, chlorinated solvents, acetonitrile, acetone, and DMSO. Yield 0.141 g, 80%. *Mp* 315 °C (dec). Anal. Calcd. for $C_{28}H_{42}AgN_6O_3PS$: C, 49.34; H, 6.21; N, 12.33; S, 4.70. Found: C, 49.37; H, 6.62; N, 12.20; S, 5.16%. Λ_M (CH_3CN, 298 K, 10^{-3} mol/L) 2.9 S cm^2 mol^{-1}. IR (KBr, cm^{-1}): 3162w, 3124w, 3109w ν(C$_{arom}$−H), 2930 m, 2854 m, 1522s ν(C═N), 1445 m, 1430 m, 1398 m, 1320 m, 1267vs, 1248vs, 1200 m, 1045vs ν(SO_3), 1096s ν(ring), 857s, 843s ν(C−N), 625s, 612 ν(C−S), 515s, 473 m, 459 m, 407 m ν(PCy_3). ^{1}H NMR ($CDCl_3$, 298 K): δ, 1.25−1.84 m br (33H, P-(C$_6H_5$)$_3$) 6.42dd (3H, 4-H (pz)), 7.64d (3H, 3,5-H (pz)), 8.01d (3H, 3,5-H (pz)). ^{1}H NMR ($CDCl_3$, 273 K): δ, 1.25−1.84 m br (33H, P-(C$_6H_5$)$_3$) 6.42dd (3H, 4-H (pz)), 7.64d (3H, 3,5-H (pz)), 8.01d (3H, 3,5-H (pz)). ^{1}H NMR ($CDCl_3$, 253 K): δ, 1.25−1.84 m br (33H, P-(C$_6H_5$)$_3$) 6.42dd (3H, 4-H (pz)), 7.64d (3H, 3,5-H (pz)), 8.01d (3H, 3,5-H (pz)). ^{1}H NMR ($CDCl_3$, 233 K): δ, 1.25−1.84 m br (33H, P-(C$_6H_5$)$_3$) 6.42dd (3H, 4-H (pz)), 7.64d (3H, 3,5-H (pz)), 8.01d (3H, 3,5-H (pz)). ^{13}C NMR (acetone-d_6, 298 K): δ, 27.0d, 27.8d, 32.0d, 32.5d (C$_{cy}$), 107.5s (C4$_{pz}$), 134.9 (C5$_{pz}$), 142.6s (C3$_{pz}$). ^{31}P{^{1}H} NMR ($CDCl_3$, 298 K): δ, 42.6dd (^1J(^{31}P-^{109}Ag): 753 Hz); (^1J(^{31}P-^{107}Ag): 653 Hz). ^{31}P{^{1}H} NMR (Acetone-d_6, 298 K): δ, 44.2dd (^1J(^{31}P-^{109}Ag): 748 Hz); (^1J(^{31}P-^{107}Ag): 648 Hz). ^{19}F{^{1}H} NMR (DMSO-d_6, 298 K): δ, −148.7. ^{19}F{^{1}H} NMR (D_2O, 298 K): δ, −150.1. ESI$^+$-MS (CH_3CN) *m*/*z* (%) = 190 [Ag(CH_3CN)$_2$]$^+$, 429 [Ag(PCy_3)(CH_3CN)]$^+$, 591 [(Ag)$_2$(Tpms)(CH_3CN)$_2$]$^+$, 687 [Ag(PCy_3)$_2$(H_2O)]$^+$, 1070 [(Ag)$_2$(Tpms)(PCy_3)$_2$]$^+$.

[Ag(PTA)(MeOH)][BF$_4$] (**4**). $AgBF_4$ (0.050 g, 0.26 mmol) was dissolved in methanol (20 mL), and the solution stirred for 30 min, then PTA (0.041 g, 0.26 mmol) was added. The resulting suspension was stirred at r.t. for 1 h, then the solid was filtered off, washed with methanol and dried under vacuum giving a grayish powder of **4**. It is soluble in water, acetonitrile, acetone, and DMSO. Yield 0.089 g, 90%. *Mp* 208 °C (dec.). Anal. Calcd. for $C_7H_{16}AgBF_4N_3OP$: C, 21.90; H, 4.20; N, 10.95. Found: C, 21.61; H, 4.23; N, 11.26%. Λ_M (H_2O, 298 K, 10^{-3} mol/L) 98.7 S cm^2 mol^{-1}. IR (KBr, cm^{-1}): 3553 m ν(O−H), 3157w ν(C−H), 1674 m δ(O−H), 1288 m, 1234s, 950vs ν(PTA), 1052vs, 1035vs, 1024vs, 1004s ν(BF_4). ^{1}H NMR (D_2O, 298 K): δ, 4.27s (6H, PCH_2N, PTA), 4.65d and 4.77d (6H, J_{AB} = 13 Hz, NCH^AH^BN, PTA). ^{31}P{^{1}H} NMR (D_2O, 298 K): δ, −77.9vbr. ^{31}P{^{1}H} NMR (D_2O, 278 K): δ, −78.6s br. ESI$^+$-MS (H_2O) *m*/*z*: 283 [Ag(PTA)(H_2O)]$^+$, 422 [Ag(PTA)$_2$]$^+$. ESI$^+$-MS (CH_3CN) *m*/*z*: 306 [Ag(PTA)(CH_3CN)]$^+$ 422 [Ag(PTA)$_2$]$^+$.

[Ag(Tpms)(PTA)] (**5**). To a solution of $AgBF_4$ (0.050 g, 0.26 mmol) in methanol (20 mL) was added Li(Tpms) (0.077 g, 0.26 mmol) and after 30 min, PTA (0.036 g, 0.25 mmol). The resulting suspension was stirred at r.t. for 3 h. The solid was filtered off, washed with several small portions of methanol and dried under vacuum giving a grayish-brown powder of **5**. It can also be obtained by using water as solvent. It is soluble in DMSO and water, slightly soluble in acetonitrile and acetone. Yield 0.074 g, 50%. *Mp* 216−218 °C. Anal. Calcd. for $C_{16}H_{21}AgN_9O_3PS\cdot$MeOH: C, 34.59; H, 4.27; N, 21.35; S, 5.43. Found: C, 34.33; H, 4.12; N, 21.08; S, 5.72%. Λ_M (DMSO, 298 K, 10^{-3} mol/L) 1.1 S cm^2 mol^{-1}. IR (KBr, cm^{-1}): 3610w, 3545w ν(O−H), 3146w ν(C$_{arom}$−H), 1640w δ(O−H), 1522 m ν(C═N), 1426 m, 1392 m, 1324 m, 1283 m, 1241sh, 1227vs, 1052vs ν(SO_3), 1095s ν(ring), 1285 m, 1270 m, 957s, 949s ν(PTA), 861s, 848 m ν(C−N). ^{1}H NMR (DMSO-d_6, 298 K): δ, 4.23s (6H, PCH_2N, PTA), 4.42d and 4.59d (6H, J_{AB} = 15 Hz, NCH^AH^BN, PTA), 6.46s br (3H, 4-H (pz)), 7.64s br (3H, 3,5-H (pz)), 8.08s br (3H, 3,5-H (pz)). ^{1}H NMR (CD_3CN, 298 K): δ, 4.24d (6H, PCH_2N, PTA), 4.50d and 4.60d (6H, NCH^AH^BN,PTA), 6.49dd (3H, 4-H (pz)), 7.71d (3H, 3,5-H (pz)), 8.12d (3H, 3,5-H (pz)). ^{13}C NMR (CD_3CN, 298 K): δ, 51.46d (C$_{PTA}$), 73.66 (C$_{PTA}$), 107.96 (C4$_{pz}$), 134.96s (C5$_{pz}$), 143.16 (C3$_{pz}$).^{31}P{^{1}H} NMR (DMSO-d_6, 298 K): δ, −84.4s br. ESI$^+$-MS (CH_3CN) *m*/*z*: 190 [Ag(CH_3CN)$_2$]$^+$, 591 [(Ag)$_2$(Tpms)(CH_3CN)$_2$]$^+$, 707 [(Ag)$_2$(Tpms)(CH_3CN)(PTA)]$^+$, 823 [(Ag)$_2$(Tpms)(PTA)$_2$]$^+$.

X-ray Crystallography of Compounds 2, 3, and 5. *X-ray Crystal Structure Determinations.* The X-ray diffraction data of **2**, **3**, and **5** were collected using a Bruker AXS-KAPPA APEX II diffractometer with graphite monochromated Mo−Kα radiation. Data were collected using ω scans of 0.5° per frame, and a full sphere of data was obtained. Cell parameters were retrieved using Bruker SMART software and refined using Bruker SAINT[36] on all the observed reflections. Absorption corrections were applied using SADABS.[36] Structures were solved by direct methods using the SHELXS−97 package[37a] and refined with SHELXL-97.[37b] Calculations were performed with the WinGX System-Version 1.80.03.[38] All hydrogens were inserted in calculated positions. Least square refinements with anisotropic thermal motion parameters for all the non−hydrogen atoms and isotropic for the remaining atoms were employed. There are disordered solvent molecules in the structure of complex **5**; PLATON/SQUEEZE[39] was used to correct the data.

Crystallographic data have been deposited at the CCDC and allocated the deposition numbers CCDC 837589−837591.

Antimicrobial Activity. *Bacterial Strains.* Silver derivatives were tested against a panel of microorganisms including *Staphylococcus aureus* ATCC 25923, *Escherichia coli* ATCC 25922, *Pseudomonas aeruginosa* ATCC 27853, *Streptococcus pneumoniae* ATCC 49619, *Enterococcus faecalis* ATCC 29212, *Streptococcus pyogenes* SF370, *Streptococcus sanguinis* SK36, *Streptococcus mutans* UA159, *Candida albicans* ATCC 24433. Bacterial strains were cultured overnight at 37 °C (*Streptococcus spp* in 5% CO_2 atmosphere) in blood agar plates with the exception of Candida that was grown in RPMI1640.

Disc Diffusion Method. Antibiotic susceptibility testing was performed by the paper disk diffusion method.[40] Growth media used for the antimicrobial assay were as indicated by the international guidelines of the CLSI.[41] Briefly, a suspension of 10^8 cells per mL prepared in saline (10^6 per mL for Candida) was spread on the solid media plates using a sterile cotton swab. Sterile filter paper discs (6 mm in diameter) were placed on the surface of inoculated plates and spotted with 20 μL of each silver derivative with a concentration of 1 mg/mL (0.1%). Each silver derivative was dissolved in DMSO. The plates were incubated for 18 h at 35 °C (*Streptococcus spp* in 5% CO_2 atmosphere). The diameters of zone inhibition (including the 6 mm disk) were measured with callipers. A reading of more than 6 mm indicated growth inhibition. No zone inhibition was observed using DMSO alone. Silver nitrate was used for comparison.

DNA Binding Study by Fluorescence Spectroscopy. UV−vis absorbance values were measured on a Varian cary-1 spectrophotometer in 10 mM phosphate buffer (pH 7.0) containing 50 mM NaCl at r.t. (25 °C). A stock solution of ct-DNA was prepared by dissolving the solid material in the same phosphate buffer. The concentration of DNA was determined by UV absorbance at 260 nm using the molar absorption coefficient ε = 260 (6600 M^{-1} cm^{-1}).[42] The competitive binding experiment was carried out by maintaining the EB and ct-DNA concentration at 5 μM and 55.7 μM, respectively, while increasing the concentration of the Ag complex (Ag-X). The fluorescence spectra of a series of solutions with various concentrations of the silver derivative and a constant EB-c-DNA complex were measured. All the fluorescence data are corrected for absorption of exciting and emitted light according to the relationship (eq 1):[17]

$$F_c = F_m \times e(A_1 + A_2)/2 \quad (1)$$

where F_c and F_m are the corrected and measured fluorescence, respectively. A_1 and A_2 are the values of absorbance of silver derivatives at the exciting and emission wavelengths. Fluorescence quenching spectra were recorded using an ISS-Greg 200 spectrofluorophotometer with an excitation wavelength of 500 nm and emission spectrum at 520−700 nm. For fluorescence quenching experiments, the Stern−Volmer's eq 2 was used:[43]

$$F_0/F = 1 + k_Q\tau_0[\text{Ag-X}] = 1 + K_{SV}[\text{Ag-X}] \quad (2)$$

where F_0 and F represent the fluorescence intensity in the absence and in the presence of drug. [Ag-X] is the concentration of the silver derivative and K_{SV} is the Stern−Volmer constant which is equal to $k_Q \times \tau_0$, where k_Q is the bimolecular quenching rate constant and τ_0 is the average fluorescence lifetime of the fluorophore in the absence of drug.

Antiproliferative Activity. *MTT Cytotoxicity Assay.* A375 cells (human malignant melanoma) were cultured in Dulbecco's Modified Eagle's Medium (DMEM) with 2 mM L-glutamine, 100 IU/mL penicillin, 100 μg/mL streptomycin, and supplemented with 10% heat inactivated fetal bovine serum (HI-FBS). Cells were cultured in a humidified atmosphere at 37 °C in presence of 5% CO_2. Briefly, cells were seeded at the initial density of 2 × 10^4 cells/mL in 96-well microtiter plates (Iwaki, Tokyo, Japan). After incubation for 24 h at 37 °C, cells were treated with different concentrations of silver derivatives **1**−**5** ranging from 0.01 μM to 100 μM and incubated for 72 h. The cell viability was assessed through an MTT (3-(4,5-dimethylthiozol-2-yl)-2,5-diphenyl-tetrazolium bromide; Sigma, St. Louis, MO) conversion assay as described.[13,44] The optical density of each sample was measured with a microplate spectrophotometer reader Titertek Multiscan microElisa (Labsystems, Helsinki, Finland) at 540 nm. Cytotoxicity is expressed as the concentration of compound inhibiting cell growth by 50% (IC_{50}). The IC_{50} values were determined using the GraphPad Prism 4 computer program (GraphPad Software, San Diego, CA, U.S.A.). $AgNO_3$ was used as comparison compound.

Scheme 1

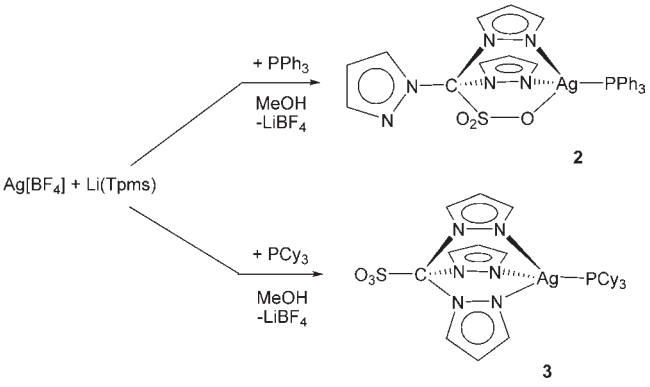

RESULTS AND DISCUSSION

Synthesis and Spectral Characterization of the Silver Complexes 1−5. The complex [Ag(Tpms)] (**1**) has been synthesized by reaction of the lithium salt of tris(pyrazol-1-yl)-methanesulfonate, Li(Tpms), with $AgBF_4$ in methanol, at r.t.. **1** is a grayish-rose solid, stable in air, poorly soluble in DMSO and acetonitrile, suggesting an oligomeric or a polymeric structure, where SO_3 and pyrazolyl rings of Tpms could be involved in coordination to silver atoms, a feature previously observed in binary M(Tpms) derivatives.[30a,d,45] **1** is a nonelectrolyte in DMSO, and the existence of silver−Tpms interactions in this solvent is also confirmed by proton NMR spectroscopy. The presence of a unique set of resonances for the H atoms of Tpms in the ^{1}H NMR of **1** in DMSO-d_6 suggests a N_3-coordination to silver, but we cannot exclude a dissociation of the polymeric solid **1** upon dissolution in polar DMSO, which can cause breaking of $SO_3\cdots$Ag interactions eventually present in the solid compound. The IR spectrum of **1** displays the expected ν(C═N + C═C) of the pyrazolyl rings at 1522 cm^{-1}, together with several bands likely due to the SO_3 group vibration modes at 1268, 1251, 1199, 1061, 1056, and 1046 cm^{-1}.[45] Additionally, three absorptions at 866, 857, and 847 cm^{-1} are assigned to ν(C−N), the former at 866 cm^{-1} having about half the intensity of the latter ones, likely indicating the presence of both coordinated and uncoordinated pyrazolyl rings, as recently proposed by Kläui et al.:[45] their "IR criterion"[45] for the assignment of the coordination mode of a similar Tpms^{tBu} ligand (Tpms^{tBu} = tris(3-*tert*-butylpyrazol-1-yl)methanesulfonate) is in fact based on the presence of a ν(C−N) band of coordinated pyrazolyl rings at about 855 cm^{-1} for N_3-coordinated Tpms^R ligands, whereas a band at 865 cm^{-1} should also be observed in the presence of uncoordinated pyrazolyl ring, as it is the case of N_2O-coordination. The positive ESI-MS spectrum of **1** in acetonitrile shows isotopic clusters centered at m/z 149 and 190 due to

Scheme 2

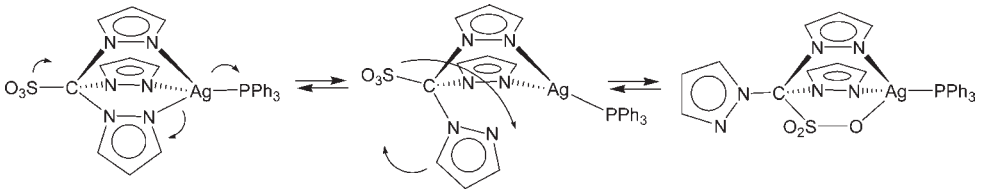

Scheme 3

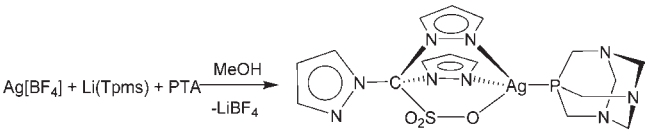

5

$[Ag(MeCN)]^+$ and $[Ag(MeCN)_2]^+$, respectively, together with peaks at m/z 550 and 591, due to $[(Ag)_2(Tpms)(MeCN)]^+$ and $[(Ag)_2(Tpms)(MeCN)_2]^+$, while in the negative ESI-MS spectrum the peaks at m/z 694 and 1096 are assigned to $[Ag(Tpms)_2]^-$ and $[(Ag)_2(Tpms)_3]^-$, in accordance with the presence in solution of mononuclear silver species but also of aggregates containing two silver centers.

Complexes $[Ag(Tpms)(PPh_3)]$ (**2**) and $[Ag(Tpms)(PCy_3)]$ (**3**) have been prepared in methanol at r.t. by reaction of Li(Tpms) with $AgBF_4$ in the presence of an equivalent amount of the appropriate phosphane (Scheme 1).

They are air-stable solids, well-soluble in water, acetonitrile, acetone, DMSO, alcohols, and chlorinated solvents. In the IR spectra of **2** and **3**, ν(C═C) and ν(C═N) of the pyrazolyl rings are observed in the range 1624−1521 cm^{-1}, whereas ν(SO), ν(pz), ν(C−N), and ν(C−S) are detected in the range 1300−600 cm^{-1}.[45] Strong bands between 550 and 400 cm^{-1} confirm the presence of coordinated PPh_3 and PCy_3.[46]

The r.t. ^1H NMR spectra of **2** and **3** show the pyrazolyl and phosphane proton resonances always deshielded with respect to those in the free ligands. The presence of a unique set of resonances for each group could be in favor of a N_3-coordination of Tpms, but, although this is in accordance with the solid state molecular structure of **3**, it contrasts with the structure of **2** containing instead a N_2O-bonded Tpms ligand (see below X-ray diffraction studies). On the basis of this evidence, we have decided to run ^1H NMR spectra in deutero-acetone and CD_2Cl_2 at low temperatures, and we have observed for **2** a progressive broadening of the H resonances of Tmps and splitting into two sets with integral ratios 2:1 below −70 °C, in accordance with a fluxionality operating in solution between silver species containing N_3- and N_2O-bonded Tpms at r.t.. This behavior has been recently observed also for similar copper(I) Tpms phosphane-compounds.[30b] However, for our silver complexes the fluxionality persists well below the temperature of −70 °C for which two quite well-resolved sets of resonances were observed in analogous copper(I) derivatives. The r.t. $^{31}P\{^1H\}$ NMR spectrum in $CDCl_3$ of **2** exhibits a doublet at δ 16.5, with $^1J(^{31}P-Ag)$ = 696 Hz, while for **3** a well resolved double doublet at δ 42.6, with $^1J(^{31}P\text{-}^{109}Ag)$ = 753 Hz and $^1J(^{31}P\text{-}^{107}Ag)$ = 653 Hz, is observed. The variable temperature $^{31}P\{^1H\}$ NMR study of our acetone-d_6 solution of **2** was also carried out: at r.t. a broad doublet at 16.9 ppm ($^1J(^{31}P\text{-}Ag)$ = 688 Hz) is detected, while on cooling at −10 °C a well resolved double doublet at 16.4 ppm arises ($^1J(^{31}P\text{-}^{109}Ag)$: = 775 Hz; $^1J(^{31}P\text{-}^{107}Ag)$ = 674 Hz). At −70 °C it shifts to 15.4 ppm (with a lowering of the silver−phosphorus coupling constants: $^1J(^{31}P\text{-}^{109}Ag)$ = 737 Hz; $^1J(^{31}P\text{-}^{107}Ag)$ = 638 Hz) and broadens. Finally, at −90 °C three broad double doublets are observed at δ 15.8 ($^1J(^{31}P\text{-}^{109}Ag)$ = 745 Hz; $^1J(^{31}P\text{-}^{107}Ag)$ = 650 Hz), 15.1 ($^1J(^{31}P\text{-}^{109}Ag)$ = 786 Hz; $^1J(^{31}P\text{-}^{107}Ag)$ = 686 Hz) and 13.1 ($^1J(^{31}P\text{-}^{109}Ag)$ = 713 Hz; $^1J(^{31}P\text{-}^{107}Ag)$ = 616 Hz), the latter with half the intensity of the former ones. This behavior supports the existence of at least three silver−phosphorus species in solution such as those depicted in the Scheme 2, the Tpms likely acting as N_3-, N_2O-, or N_2-donor.

The positive ESI-MS spectrum of **2** in acetonitrile is characterized by clusters centered at m/z 632, 686, and 1034 due to $[Ag(PPh_3)_2]^+$, $[Ag(Tpms)(PPh_3)Na]^+$, and $[(Ag)_2(Tpms)(PPh_3)_2]^+$ species, respectively. The positive ESI-MS of **3** in acetonitrile shows peaks at 190 ($[Ag(CH_3CN)_2]^+$), 429 ($[Ag(PCy_3)(CH_3CN)]^+$), 591 ($[(Ag)_2(Tpms)(CH_3CN)_2]^+$), 687 ($[Ag(PCy_3)_2(H_2O)]^+$), and 1070 $[(Ag)_2(Tpms)(PCy_3)_2]^+$.

By treatment of a MeOH solution of $AgBF_4$ with PTA at r.t., $[Ag(PTA)(MeOH)][BF_4]$ (**4**) is obtained, as a high melting brown powdered solid, soluble in water, acetonitrile, acetone, and DMSO. The conductivity measurement of a water solution of **4** exhibits a Λ_M value of 98.7 S cm^2 mol^{-1}, close to those reported for 1:1 electrolytes in water (118−131 S cm^2 mol^{-1})[47], in accordance with an extensive dissociation. The IR spectrum of **4** confirms the presence of both the coordinated PTA ligand[30b] and the $[BF_4]^-$ group.[48a] In detail, the band at about 1050 cm^{-1}, because of this counterion, displays a fine splitting, indicative of its involvement in interactions with Ag through F atoms. We can hypothesize a polymeric structure for **4** where both $[BF_4]^-$ and PTA could play the role of bridging ligands.[30k,l,49] The ^1H NMR spectrum of **4** in D_2O shows two types of methylene protons, typical of the PTA ligand. One of them, assigned to the P−CH_2−N moiety, occurs as a singlet at δ 4.27 whereas the other one, corresponding to the N−CH_2−N group, displays an AB spin system centered at δ 4.73 (J_{AB} = 13 Hz), attributed to the N−CH_{ax}−N and N−CH_{eq}−N protons.[30b] The $^{31}P\{^1H\}$ NMR spectrum exhibits a broad singlet at δ −77.9, the $^{107}Ag-^{31}P$ and $^{109}Ag-^{31}P$ spin−spin coupling not being observed because of the fast ligand exchange.[30k,50] The ESI-MS spectra of **4** carried out in water and acetonitrile show peaks due to silver species always containing the PTA ligand. The ionic dissociation of **4** in ionizing solvents is further confirmed by the ^{19}F NMR spectrum of **4** in D_2O and DMSO, typical of a ionic BF_4 group.[48b]

Finally, by reaction of a methanol solution of $AgBF_4$ with Li(Tpms) and PTA at r.t., the derivative $[Ag(PTA)(Tpms)]$ (**5**) has been isolated (Scheme 3). Because of stronger coordination ability of PTA to Ag(I) in comparison with Tpms, to prevent

dx.doi.org/10.1021/ic201714c |*Inorg. Chem.* 2011, 50, 11173–11183

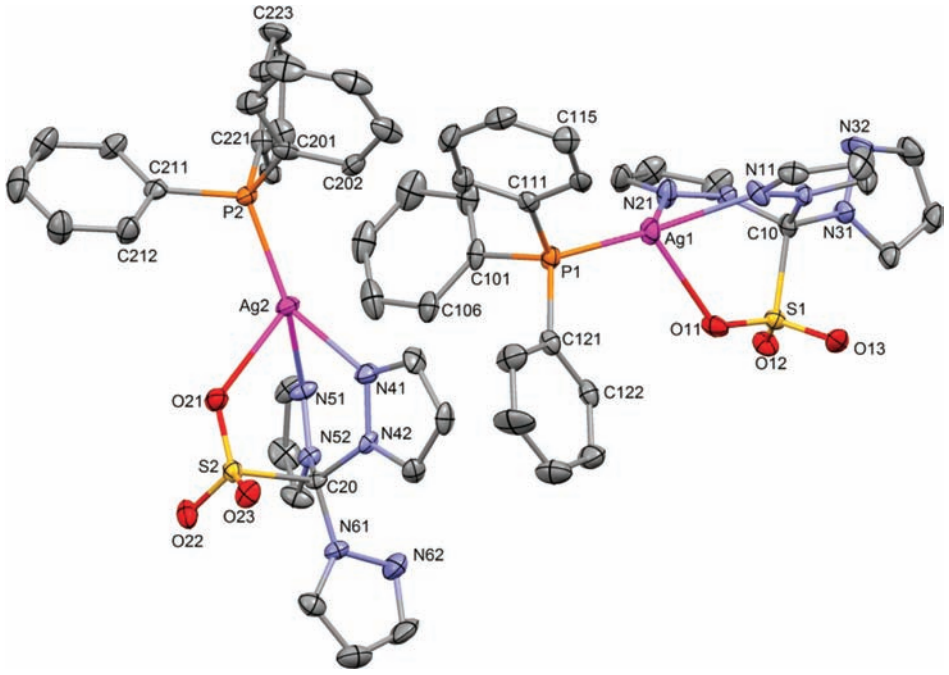

Figure 2. Ortep diagram of [Ag(Tpms)(PPh_3)] (**2**), drawn at 50% probability. Hydrogen atoms and chloroform molecule were ommitted for clarity. Selected bond distances (Å) and angles (deg): P1−Ag1 2.3286(10), P2−Ag2 2.3259(12), O11−Ag1 2.551(3), O21−Ag2 2.513(3), N11−Ag1 2.259(4), N21−Ag1 2.307(4), N41−Ag2 2.307(4), N51−Ag2 2.282(4), N11−N12 1.367(4), N21−N22 1.360(4), N31−N32 1.356(5), N51−N52 1.350(5); N11−Ag1−N21 79.41(13), N11−Ag1−P1 147.14(10), N21−Ag1−P1 130.53(10), N11−Ag1−O11 78.31(12), N21−Ag1−O11 74.68(12), P1−Ag1−O11 118.52(7), N51−Ag2−N41 78.14(14), N51−Ag2−P2 141.36(10), N41−Ag2−P2 137.60(10), N51−Ag2−O21 78.56(12), N41−Ag2−O21 77.10(12), P2−Ag2−O21 117.41(7), N31−C10−N12 107.8(4), N31−C10−N22 107.1(4), N12−C10−N22 112.7(4), N61−C20−N52 107.7(3), N61−C20−N42 107.2(3), N52−C20−N42 112.3(3).

cleavage Ag−N(Tpms) bond, addition of PTA to the reaction mixture should be slow, after reaction of Tpms with Ag(I) center and in lower amount than stoichiometric, to yield **5** in high purity.

We have tried to apply the "IR criterion" of Kläui et al.[45] also to our Tpms derivatives with phosphanes, but it appears not to be valid for our compounds **2**, **3**, and **5**. In fact, in their IR spectra we have always detected two ν(C−N) absorptions, in spite of the different solid state N_2O- (in **2** and **5**) and N_3-coordination modes of Tpms (in **3**), as shown (see below) by X-ray diffraction studies. On the other hand, the criterion based on the number of IR active sulfonate vibrations[51] is not straightforward. Capwell states that a "free" sulfonate (C_{3v} symmetry) should exhibit only two IR active vibration modes, whereas a coordinated one (C_s symmetry) should instead exhibit at least three bands.[51a] In the IR of **2**, **3**, and **5** at least three bands are always observed in the ranges expected for the vibration modes of the SO_3^- group, indifferently to its free or silver-coordinated nature.

The r.t. ^{1}H NMR spectrum of **5** in DMSO-d_6 similarly to **4**, shows two types of methylene protons for the coordinated PTA. One of them, occurs as a singlet at 4.23 ppm while the second one displays an AB spin system centered at 4.50 ppm (J_{AB} = 15 Hz).[30b] Similarly to the other silver Tpms derivatives, the ^{1}H NMR spectrum of **5** at r.t. reveals the presence of three equivalent pyrazolyl rings (three broad singlets at δ 8.08, 7.64, and 6.46 corresponding to the pyrazolyl protons in positions 5, 3 and 4). The r.t. $^{31}P\{^1H\}$ NMR spectrum, equally to **4**, exhibits a broad singlet at δ −84.4, and no $^{107}Ag-^{31}P$ or $^{109}Ag-^{31}P$ spin−spin coupling was observed, likely because of the fast ligand exchange.[50] This effect was previously reported for other PTA-Ag(I) complexes.[30k]

The positive ESI-MS spectrum in acetonitrile of **5** shows peaks at m/z 190 ($[Ag(CH_3CN)_2]^+$), 591 ($[(Ag)_2(Tpms)(CH_3CN)_2]^+$), 707 ($[(Ag)_2(Tpms)(CH_3CN)(PTA)]^+$), and 823 ($[(Ag)_2(Tpms)(PTA)_2]^+$), in accordance with possible aggregation in solution and formation of dinuclear species.

X-ray Diffraction Studies of Silver Compounds 2, 3, and 5. X-ray quality crystals of **2**, **3**, and **5** were obtained from chloroform (**2**, **3**) or methanol (**5**) solutions. Ortep diagrams are shown in Figures 2−4 with selected bond distances and angles listed in the respective legends. Crystallographic data are presented in Table 1. In the structure of **2** there are two molecules of the silver complex apart from a $CHCl_3$ solvent molecule, probably because of conformational differences as depicted in the Supporting Information, Figure S1. In the structures of **3** and **5** the asymmetric unit comprises only one of the entire complex entities.

All these complexes have four-coordinate, highly distorted tetrahedral silver atoms. The Tpms ligand coordinates to silver in κ^3-N_2O (**2** and **5**) or κ^3-N_3 (**3**) fashion; the fourth coordination positions are occupied by the P atoms of the phosphanes. Houser et al.[52] introduced a parameter (τ_4) to describe the geometry of a four-coordinate metal system which is determined by the equation

$$\tau_4 = [360° - (\beta + \alpha)]/141°$$

where β and α are the largest angles involving the metal. By means of this simple criterium, perfect square planar or tetrahedral geometries should have τ_4 values of 0 or 1, respectively. For our complexes such a parameter assumes values of 0.58 and 0.57 (**2**), 0.62 (**3**) or 0.53 (**5**), thus showing that the structures are distorted tetrahedral. The distortions result from the

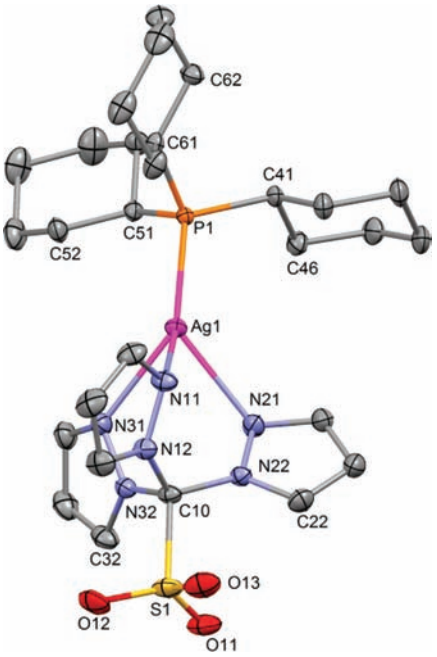

Figure 3. Ortep diagram of [Ag(Tpms)(PCy_3)] (**3**), drawn at 50% probability. Hydrogen atoms were ommitted for clarity. Selected bond distances (Å) and angles (deg): P1−Ag1 2.3555(4), N11−Ag1 2.4058(14), N21−Ag1 2.4137(13), N31−Ag1 2.3848(14), N11−N12 1.3627(19), N21−N22 1.3571(18), N31−N32 1.3614(18); N11−Ag1−N21 77.44(5), N31−Ag1−N11 76.86(5), N31 Ag1−N21−75.74(5), P1−Ag1−N11 138.98(3), P1−Ag1−N21 130.03(3), P1−Ag1−N31 133.28(4), N22−C10−N12 109.39(13), N32−C10−N12 109.80(12), N32−C10 N22−109.99(12).

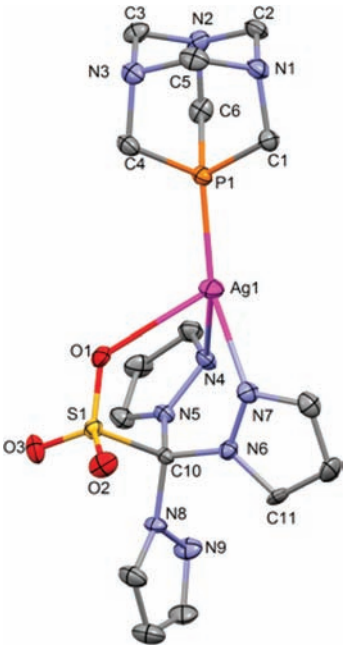

Figure 4. Ortep diagram of [Ag(Tpms)(PTA)] (**5**), drawn at 50% probability. Hydrogen atoms were ommitted for clarity. Selected bond distances (Å) and angles (deg): P1−Ag1 2.3431(14), O1−Ag1 2.607(4), N4−Ag1 2.477(5), N7−Ag1 2.256(5) N4−N5 1.360(6), N6−N7 1.379(6), N8−N9 1.374(6); P1−Ag1−N4 139.49(11), P1−Ag1−N7 145.98(12), N4−Ag1−N7 73.46(15), N6−C10−N8 108.9(4), N5−C10−N8 109.2(4), N56−C10−N6 110.7(4).

chelation of the Tpms ligand, which shows bite angles in the ranges of 74.7−79.4° (**2**), 75.7−77.4°(**3**), and 73.4−79.4° (**5**). The Ag−N bond distances adopt values of 2.259(4)−2.307(4) Å (**2**), 2.3848(14)−2.4137(13) (**3**), and 2.256(5)−2.477(5) Å (**5**). These distances compare well with those found in other pseudo tetrahedral silver complexes, for example, with bis(pyrazolyl)alkane ligands such as in [Ag{$RR'C(pz)_2$}$_2$]X (R = R′ = Ph; R = H, R′ = Ph; R = H, R′ = CH_2Ph; X = PF_6.[53] R = R′ = Me, X = ClO_4[54]), with the bitopic bis(pyrazolyl)-methane ligands as in [$Ag_2(\mu$-L)$_2$]X_2 (L = $CH(pz)_2(CH_2)_2CH(pz)_2$ or $CH(pz)_2(CH_2)_3CH(pz)_2$; X = BF_4 or CF_3SO_3)[55] or even with the multitopic 1,2,4,5-$C_6H_2[CH_2OCH_2CH(pz)_2]_4$ ligand;[56] in all cases, the Ag−N bond distances are in the 2.234(2)−2.5092(19) Å range.

The P−Ag bond distances, in the 2.3259(12)−2.3555(4) Å range, are considerably shorter than those usually found in both neutral[57] or cationic[58] silver phosphane complexes and even shorter than that in the T-shaped three-coordinate complex [Ag{$P(C_6H_4CH_2NMe_2$-2)$_3$}(OCOCF$_3$)].[59] Moreover, the O−Ag bond distances, ranging from 2.513(3) to 2.607(4) Å in our complexes, are much longer than the normal covalent silver(I)−oxygen bond length of about 2.3 Å indicating that the sulfonate arms in **2** and **5** are only weakly bonded to the metal.

Although the pyrazolyl rings in our structures are all nearly planar, the silver atoms lie out of these planes [average values of 1.810 (**5**), 1.352 (**3**), and 0.417 and 0.199 Å (**2**), and considering only the coordinated rings] with the Ag−N−N−C_{pyr} torsion angles averaging 167.5, 141.1, and 140.2° for **2**, **3**, and **5**, respectively. (Table 2). These angles would be 180° in the absence of tilting. The consideration of the Ag−N−N−$C_{methine}$ torsion angles, as proposed by Templeton et al.,[60] is an alternative for measuring such distortions, and would equal 0° for an undistorted geometry. For **3** and **5** such angles (Table 2) are opposite in sign and considerably greater than those for **2**, therefore reinforcing the fact that the metal atom is considerably away from the planes of the pyrazole rings in the former cases. Moreover, in both molecules of **2** the methine carbon is away (though very slightly) from such planes, in contrast to structures **3** and **5**. The somewhat unexpected (because of the way the ligand coordinates to the metal) higher degree of tilting of complex **3** is shown in the Supporting Information, Figure S2. It is in **3**, however, that the P−Ag−C_{sp3} angle is higher (174.85°), averaging 166.12° in complex **2** and equal to 160.21° in **5**. Despite those discrepancies, the N−C_{sp3}−N angles, which should reflect the way the ligand binds to the metal, are similar in all the structures and adopt values from 109.73 (in **3**) to 112.47° (in **2**).

The degree of tilting of the pyrazolyl rings in several metal complexes has previously been related[61] to unfavorable nonbonding interactions resulting from either bulky substituents on the pyrazolyl rings or from the size of the metal atoms. In our cases, we have tentatively related several structural parameters with the cone angles of the phosphanes[61] and summarized them in Table 2. Taking into account that the mode of coordination of the scorpionate ligand in **2** and **5** differs from that in **3**, it appears that for the former cases (κ^3-NNO coordination type) a smaller cone angle of the phosphane gives rise to smaller $AgNNC_{pz}$ torsion angles, shorter intraligand $N_{coord}\cdots N_{coord}$, but longer metal-N distances. Therefore, the pyrazolyl rings of

dx.doi.org/10.1021/ic201714c |*Inorg. Chem.* 2011, 50, 11173–11183

Table 1. Crystallographic Data for Compounds [Ag(Tpms)(PPh$_3$)] (2), [Ag(Tpms)(PCy$_3$)] (3), and [Ag(Tpms)(PTA)] (5)

	2·CHCl$_3$	3	5
empirical formula	2($C_{28}H_{24}AgN_6O_3PS$), $CHCl_3$	$C_{28}H_{42}AgN_6O_3PS$	$C_{16}H_{21}AgN_9O_3PS$
formula weight	1446.23	681.58	558.32
crystal system	orthorhombic	monoclinic	orthorhombic
space group	*P*212121	*P*21/*n*	*Pbca*
a (Å)	13.0005(5)	12.6027(3)	7.1753(7)
b (Å)	21.2408(10)	15.1631(5)	15.0485(12)
c (Å)	21.7244(9)	16.2546(5)	41.898(4)
β (deg)	90	104.472(2)	90
V (Å^3)	5999.0(4)	3007.63(15)	4524.1(7)
Z	4	4	4
density (calculated) (Mg/m^3)	1.601	1.505	1.639
absorption coefficient (mm^{-1})	0.970	0.833	1.092
F(000)	2920	1416	2256
reflections collected/unique	59812/13212 [*R*(int) = 0.0905]	45299/12082 [*R*(int) = 0.0408]	35133/4123 [*R*(int) = 0.0845]
goodness-of-fit on F^2	1.000	0.964	1.004
final *R* indices [$I > 2\sigma(I)$]	R_1 = 0.0451, wR_2 = 0.0700	R_1 = 0.0341, wR_2 = 0.0745	R_1 = 0.0519, wR_2 = 0.1439

Table 2. Some Structural Parameters of 2, 3, and 5 and the Cone Angles of the Phosphanes

	2	3	5
intraligand $N_{coord}\cdots N_{coord}$ distance (Å)	*av.* 2.965	*av.* 2.979	2.835
Ag−N−N−C_{pz} torsion angle (deg)	166.6, −170.1 (Ag1) 161.1, −172.1 (Ag2)	*av.* 141.1	*av.* 140.2
Ag−N−N−$C_{methine}$ torsion angle (deg)	1.7, −3.6 (Ag1) −5.3, −8.1 (Ag2)	*av.* 35.97	−28.4, −44.9
Ag−N (Å)	*av.* 2.288	*av.* 2.401	*av.* 2.367
phosphane cone angle (deg)	145	170	118

Table 3. Disc Diffusion Test of Compounds 1−5 against a Panel of Reference Bacterial Strains[a]

compound	*S. aureus*	*S. pyogenes*	*S. pneumonae*	*S. sanguins*	*S. mutans*	*E. faecalis*	*P. aeruginosa*	*E. coli*	*C. albicans*
1	11.0	12.0	11.0	12.0	11.0	10.0	15.0	11.0	12.0
2	6.0	6.0	6.0	6.0	6.0	6.0	6.0	6.0	6.0
3	12.0	14.0	13.0	13.0	14.0	9.0	15.0	11.0	15.0
4	14.0	15.0	15.0	14.0	14.0	9.0	17.0	13.0	17.0
5	15.0	16.0	16.0	16.0	16.0	10.0	17.0	15.0	20.0
$AgNO_3$	11.0	13.0	13.0	11.0	12.0	11.0	14.0	11.0	14.0

[a] Diameters of zone inhibition are expressed in millimeters.

the scorpionate ligand tilted to overcome unfavorable interactions from the bulky phosphane, which is further evidence of the versatility of those ligands.

Antibacterial Activity. The antimicrobial activities of the compounds **1**−**5** against bacteria and fungi were examined qualitatively by agar diffusion tests (Table 3). Whereas the lithium derivative of Tpms shows no activity, the silver derivatives possess a wide spectrum of effective antibacterial and antifungal activities. In general, compounds bearing PTA ligand (**4** and **5**) show a significantly higher antibacterial activity than silver nitrate ($P < 0.01$ by the Fisher's least significant difference procedure). Among Gram-positive bacteria, only *E. faecalis* was not significantly responding to any of the compounds. This result is not surprising in view of the well-known general tolerance toward many antibacterial agents that characterizes this species. For the two Gram-negative species tested, our results demonstrate that compound **4** is less active against *E. coli* but with a diameter of the inhibition zone still wider than that of the comparison test compound. The active compounds **4** and **5** significantly inhibit the growth of the *P. aeruginosa* strain. The recorded diameters were considerably wide (17 mm), even if a general higher susceptibility toward silver is clear from the diameter of the silver nitrate (14 mm against a mean value of 12). It is possible that *Pseudomonas* is basically more susceptible to the action of the silver ions. At last, compound **5** shows a very good activity against *C. albicans*, with a mean diameter size of 20 mm.

Fluorescence Studies. Fluorescence quenching may result from a variety of processes such as excited state reactions, energy transfer, ground state complex formation, and collisional processes. Collisional or dynamic quenching refers to a process

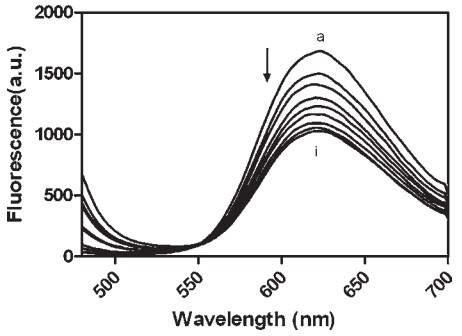

Figure 5. Fluorescence spectra of EB-DNA in the presence of compound **1** at 293 K. The total concentrations of **1** are 0, 5, 10, 15, 20, 25, 30, 40, 50 μM/L for spectra (a−i), respectively.

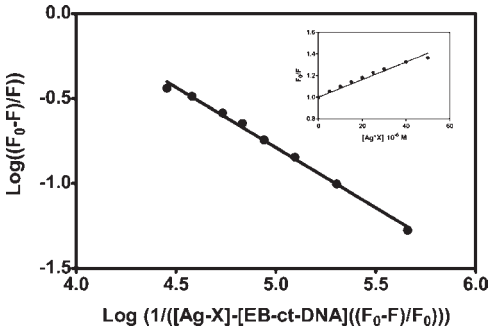

Figure 6. Plot of experimental quenching data obtained from titration plotted following eq 3. Inset: Stern−Volmer plot.

Table 4. K_{SV} and K_A Values for Binding of Compounds 1−5 with ct-DNA

compound	$K_{SV}10^3$ M^{-1}	K_A 10^4 M^{-1}	n
1	7.4(±0.38)	0.63(±.06)	0.82
2	14.9(±0.48)	5.3(±0.7)	0.93
3	3.4(±0.15)	70.7(±1.7)	0.91
4	2.71(±0.19)	0.05(±.01)	0.91
5	3.45(±0.5)	0.154(±.06)	0.62
$AgNO_3$	3.03(±.0.1)	0.148(±.02)	0.77

where the fluorophore and the quencher come into contact during the lifetime of the excited state, whereas static quenching concerns the formation of a fluorophore−quencher complex. The fluorescence spectra for the interaction of the silver compound **1** with EB-ct-DNA at 298 K are shown in Figure 5. EB-ct-DNA exhibits a strong fluorescence emission at 597 nm on excitation at 500 nm. All the tested silver complexes have negligible fluorescence under these experimental conditions. Even so, to avoid any contribution from ligands to the fluorescence of EB-ct-DNA, control sets were subtracted. Addition of silver compounds to EB-ct-DNA leads to a significant quenching of the fluorescence intensity of EB-ct-DNA. According to the Stern−Volmer eq 2,[43] for fluorescence quenching of EB-ct-DNA (in Figure 5 we report the quenching because of the binding of ct-DNA by compound **1**), F_0/F is plotted versus the quencher concentration [Ag-X] (Figure 6). The Stern−Volmer quenching constant K_{SV} was obtained by the slope of the regression curve in the linear range (inset of Figure 6). Data for the quenching constants for the interaction on all the studied Ag^+ complexes are reported in Table 4.

Generally, the linearity of the Stern−Volmer plot may have two meanings: the existence of one binding site for the ligand in the proximity of the fluorophore, or more than one binding site equally accessible to the ligand. In the case of fluorescence caused only by EB-ct-DNA and assuming that the silver derivative (1:1 stoichiometry) is responsible for the fluorescence quenching of the protein, the observed change in fluorescence of EB-ct-DNA, after binding with increasing concentrations of Ag complexes, can be related to the following eq 3:[62]

$$\log(F_0{-}F)/F = n \log K_A - n \log \{1/([\text{Ag-X}] - [\text{EB-ct-DNA}](F_0 - F)/F_0))\} \quad (3)$$

where [EB-ct-DNA] and [Ag-X] are the total concentration of EB-ct-DNA and different Ag complexes tested, respectively. On the basis of the assumption that n is equal to 1 and where any assumed conditions concerning free EB-ct-DNA or free/bound drug concentrations are not required, the plot of $\log(F_0 - F)/F$ versus $\log(1/([\text{Ag-X}] - n[\text{EB-ct-DNA}](F_0 - F)/F_0)))$ is drawn and fitted linearly, and then the slope n can be obtained.[62] Figure 6 shows the plot obtained for the compound **1**, and all values of association constants obtained for the different complexes are reported in Table 4. From the values of the K_{SV} and K_A constants, related to the binding of the different Ag^+ complexes to DNA, we can see that compounds **2** and **3** show the higher binding activity on DNA. In particular, the interaction of **3** results in about a 450 fold increase of the binding constant in comparison with that of $AgNO_3$ used as control. The binding activity on DNA follows the sequence **3** > **2** > **1** > **5** > **$AgNO_3$** > **4**.

Antineoplastic Activity. Biomedical applications of Ag^+ complexes are related mostly to their antibacterial action, which appears to involve interaction with DNA. A similar interaction of the metal with DNA may also be the cause of the antitumor action of some of those complexes. The cytotoxic activities of the Ag^+ compounds **1**−**5** as 50% inhibitory concentration (IC_{50}) values against human malignant melanoma cells (A375) are shown in Table 5 and compared with $AgNO_3$. Complexes **2** and **3** tested for in vitro cytotoxic activity present pronounced antiproliferative effects with mean IC_{50} values of 0.97 and 0.42 μM, respectively, being 2 and 4 times more active than silver nitrate. The cytotoxic activities of the other complexes are smaller than those of **2** and **3**, following the sequence **3** > **2** > **1** > **5** > **$AgNO_3$** ≫ **4**, in line with the binding activity of these complexes on DNA.

Table 5. Cytotoxic Activity (IC_{50}) of Compounds 1−5 on A375 Human Malignant Melanoma Cell Line[a]

compounds	IC_{50} /μM
1 (95% CI)	1.62 (0.87−2.65)
2 (95% CI)	0.97 (0.69−1.37)
3 (95% CI)	0.42 (0.24−0.75)
4 (95% CI)	12.35 (10.32−15.24)
5 (95% CI)	1.90 (0.75−3.26)
$AgNO_3$ (95% CI)	2.03 (1.22−3.04)

[a] The IC_{50} value is the concentration of compound that affords a 50% reduction in cell growth (after 72 h of incubation). CI = confidence interval.

CONCLUSIONS

Novel silver(I) complexes have been prepared, bearing the scorpionate ligand Tpms and also the monodentate phosphanes PPh_3, PCy_3, and PTA. In the presence of both Tpms and phosphane, compounds **2**, **3**, and **5** are obtained, existing as mononuclear species in the solid state with tetrahedral silver atoms coordinated by a phosphane and N_3-bonded (in **3**) or N_2O-ligated (in **2** and **5**) Tpms. The coordination versatility of the scorpionate ligands is also expressed by the tilting of the coordinated pyrazolyl rings which appears to be related to the cone angles of the phosphanes: the higher this parameter, the higher the $AgNNC_{pz}$ torsion angles, which can be envisaged as a way of the ligand to avoid unfavorable interactions with other bulky ligands.

Derivatives **1** and **4**, likely polynuclear in the solid state, dissociate in solution into mononuclear and dinuclear species. These silver(I) complexes display antibacterial activity which is compared with that of $AgNO_3$ used as control. Although **2** shows a lower activity, compounds bearing PTA ligand (**4** and **5**) are more active. These findings demonstrate a possible relationship between structure/activity and selectivity for silver(I) complexes, which can be further explored toward a more selective antibacterial activity.

Our silver compounds also have an antiproliferative activity, which, in the case of **2** and **3**, is two and five times, respectively, that of $AgNO_3$ used as the control (Table 3). These results are in line with the values of the binding constant (K_A) for the interaction of silver compounds with DNA (Table 4). From these data we observe that the affinities of **2** and **3** are higher than those of the other derivatives and the control ($AgNO_3$). In particular, for the interaction of the Ag complexes with DNA, we observe a very high binding activity of complex **3** (450 fold that of $AgNO_3$), the interaction of which with DNA was the object of further characterization.

ASSOCIATED CONTENT

Supporting Information. X-ray crystallographic files in CIF format for the X-ray structure determination of $\mathbf{2}\cdot{}^1/_2\mathbf{CHCl_3}$, **3**, **5**. Figures S1 and S2. This material is available free of charge via the Internet at http://pubs.acs.org.

AUTHOR INFORMATION

Corresponding Author

*E-mail: claudio.pettinari@unicam.it (C.P.), fatima.guedes@ist.utl.pt (M.F.G.d.S.), pombeiro@ist.utl.pt (A.J.L.P.), piotr.smolenski@chem.uni.wroc.pl (P.S.).

ACKNOWLEDGMENT

We thank the University of Camerino Financial Support, the Fundação para a Ciência e a Tecnologia (FCT), Portugal, and its Strategy Programme PEst-OE/QUI/UI0100/2011, and the KBN program (Grant N204 280438), Poland.

REFERENCES

(1) Guo, Z.; Sadler, P. J. *Angew. Chem., Int. Ed.* **1999**, *38*, 1512–1531.
(2) Orvig, C.; Abrams, M. J. *Chem. Rev.* **1999**, *99*, 2201–2204.
(3) Marambio-Jones, C.; Hoek, E. M. V. *J. Nanopart. Res.* **2010**, *12*, 1531–1551.
(4) (a) Klasen, H. J. *Burns* **2000**, *26*, 117–130. (b) Klasen, H. J. *Burns* **2000**, *26*, 131–138.
(5) Farrell, N. In *Comprehensive Coordination Chemistry*, 2nd ed.; McCleverty, J. A., Meyer, T. J., Eds.; Elsevier Pergamon: Oxford, U.K., 2004; Vol. 9, pp 809−840.
(6) Clement, J. L.; Jarret, P. S. *Met. Based Drugs* **1994**, *1*, 467–482.
(7) Tambe, S. M.; Sampath, L.; Modak, S. M. *J. Antimicrob. Chemother.* **2001**, *47*, 589–598.
(8) Jakupec, M. A.; Unfried, P.; Keppler, B. K. *Rev. Physiol. Biochem. Pharmacol.* **2005**, *153*, 101–111.
(9) Nomiya, K.; Takahashi, S.; Noguchi, R.; Nemoto, S.; Takayama, T.; Oda, M. *Inorg. Chem.* **2000**, *39*, 3301–3311.
(10) Kasuga, N. C.; Sugie, A.; Nomiya, K. *Dalton Trans.* **2004**, 3732–3740.
(11) Chung, J. Y.; Herbert, M. E. *West. J. Med.* **2001**, *175*, 205–206.
(12) Fuller, F. W.; Parrish, M.; Nance, F. C. *J. Burn Care Rehabil.* **1994**, *15*, 213–223.
(13) Page, M.; Bejaoui, N.; Cinq-Mars, B.; Lemieux, P. *Int. J. Immunopharm.* **1988**, *10*, 785–793.
(14) Jung, W. K.; Koo, H. C.; Kim, K. W.; Shin, S.; Kim, S. H.; Park, Y. H. *Appl. Environ. Microbiol.* **2008**, *74*, 2171–2178.
(15) Holt, K. B.; Bard, A. J. *Biochemistry* **2005**, *44*, 13214–13223.
(16) (a) Yamanaka, M.; Hara, K.; Kudo, J. *Appl. Environ. Microbiol.* **2005**, *71*, 7589–7593. (b) Jung, W. K.; Koo, H. C.; Kim, K. W.; Shin, S.; Kim, S. H.; Park, Y. H. *Appl. Environ. Microbiol.* **2008**, *74*, 2171–2178.
(17) Steiner, R. F.; Weinryb, L. *Excited states of protein and nucleic acid*; Plenum Press: New York, 1971; p 40.
(18) Fox, C. L., Jr. *Surg. Gynecol. Obstet.* **1983**, *157*, 82–88.
(19) Nomiya, K.; Tsuda, K.; Sudoh, T.; Oda, M. *J. Inorg. Biochem.* **1997**, *68*, 39–44.
(20) (a) Nomiya, K.; Tsuda, K.; Kasuga, N. C. *J. Chem. Soc., Dalton Trans.* **1998**, 1653–1660. (b) Nomiya, K.; Noguchi, R.; Oda, T. *Inorg. Chim. Acta* **2000**, *298*, 24–32. (c) Nomiya, K.; Tsuda, K.; Tanabe, Y.; Nagano, H. *J. Inorg. Biochem.* **1998**, *69*, 9–14.
(21) Bult, A.; Plug, C. M. *Anal. Profiles Drug Subst.* **1984**, *13*, 553–571.
(22) Nangia, A. K.; Hung, C. T.; Lim, J. K. C. *Drugs Today* **1987**, 21–30.
(23) (a) Deshpande, L. M.; Chopade, B. A. *Biometals* **1994**, *7*, 49–56. (b) De Wit, P. P.; Van Doorne, H.; Bult, A. *Int. J. Clin. Pharm.* **1983**, *5*, 298–301.
(24) Kawai, K.; Suzuki, S.; Tabata, Y.; Taira, T.; Ikada, Y.; Nishimura, Y. *J. Biomed. Mater. Res.* **2001**, *57*, 346–356.
(25) Bowmaker, G. A.; Effendy; Lim, K. C.; Skelton, B. W.; Sukarianingsih, D.; White, A. H. *Inorg. Chim. Acta* **2005**, *358*, 4342–4370.
(26) Bowmaker, G. A.; Effendy; Nitiatmodjo, M.; Skelton, B. W.; White, A. H. *Inorg. Chim. Acta* **2005**, *358*, 4327–4341.
(27) Bowmaker, G. A.; Effendy; Marfuah, S.; Skelton, B. W.; White, A. H. *Inorg. Chim. Acta* **2005**, *358*, 4371–4388.
(28) Di Nicola, C.; Effendy; Marchetti, F.; Nervi, C.; Pettinari, C.; Robinson, W. T.; Sobolev, A. N.; White, A. H. *Dalton Trans.* **2010**, 908–922.
(29) (a) Kläui, W.; Berghahn, M.; Rheinwald, G.; Lang, H. *Angew. Chem., Int. Ed.* **2000**, *39*, 2464–2466. (b) Kläui, W.; Schramm, D.; Peters, W.; Rheinwald, G.; Lang, H. *Eur. J. Inorg. Chem.* **2001**, 1415–1424. (c) Kläui, W.; Berghahn, M.; Frank, W.; Reiß, G. J.; Schönherr, T.; Rheinwald, G.; Lang, H. *Eur. J. Inorg. Chem.* **2003**, 2059–2070. (d) Fomitchev, D. V.; McLauchlan, C. C.; Holm, R. H. *Inorg. Chem.* **2002**, *41*, 958–966.
(30) (a) Papish, E. T.; Taylor, M. T.; Jernigan, F. E., III; Rodig, M. J.; Shawhan, R. R.; Yap, G. P. A.; Jové, F. A. *Inorg. Chem.* **2006**, *45*, 2242–2250. (b) Wanke, R.; Smoleński, P.; Guedes da Silva, M. F. C.; Martins, L. M. D. R. S.; Pombeiro, A. J. L. *Inorg. Chem.* **2008**, *47*, 10158–10168. (c) Silva, T. F. S.; Alegria, E. C. B. A.; Martins, L. M. D. R. S.; Pombeiro, A. J. L. *Adv. Synth. Catal.* **2008**, *350*, 706–716. (d) Dinoi, C.; Guedes da Silva, M. F. C.; Alegria, E. C. B. A.; Smoleński, P.; Martins, L. M. D. R. S.; Poli, R.; Pombeiro, A. J. L. *Eur. J. Inorg. Chem.*

2010, 2415–2424. (e) Smoleński, P.; Pombeiro, A. J. L. *Dalton Trans.* **2008**, 87–91. (f) Kirillov, A. M.; Smoleński, P.; Guedes da Silva, M. F. C.; Pombeiro, A. J. L. *Acta Crystallogr.* **2008**, *E64*, o496–o497. (g) Smoleński, P.; Kirillov, A. M.; Guedes da Silva, M. F. C.; Pombeiro, A. J. L. *Acta Crystallogr.* **2008**, *E64*, o556. (h) Kirillov, A. M.; Smoleński, P.; Guedes da Silva, M. F. C.; Pombeiro, A. J. L. *Acta Crystallogr.* **2008**, *E64*, m603–m604. (i) Jaremko, L.; Kirillov, A. M.; Smoleński, P.; Lis, T.; Pombeiro, A. J. L. *Inorg. Chem.* **2008**, *47*, 2922–2924. (j) Smoleński, P.; Dinoi, C.; Guedes da Silva, M. F. C.; Pombeiro, A. J. L. *J. Organomet. Chem.* **2008**, *693*, 2338–2344. (k) Lis, A.; Guedes da Silva, M. F. C.; Kirillov, A. M.; Smoleński, P.; Pombeiro, A. J. L. *Cryst. Growth Des.* **2010**, *10*, 5244–5253. (l) Kirillov, A. M.; Wieczorek, S.; Lis, A.; Guedes da Silva, M. F. C.; Florek, M.; Król, J.; Staroniewicz, Z.; Smoleński, P.; Pombeiro, A. J. L. *Cryst. Growth Des.* **2011**, *11*, 2711–2716.

(31) Liu, J. J.; Galettis, P.; Farr, A.; Maharaj, L.; Samarasinha, H.; McGechan, A. C.; Baguley, B. C.; Bowen, R. J.; Berners-Price, S. J.; McKeage, M. J. *J. Inorg. Biochem.* **2008**, *102*, 303–310.

(32) Thati, B.; Noble, A.; Creaven, B. S.; Walsh, M.; McCann, M.; Kavanagh, K.; Devereux, M.; Egan, D. A. *Cancer Lett.* **2007**, *248*, 321–331.

(33) Medvetz, D. A.; Hindi, K. M.; Panzner, M. J.; Ditto, A. J.; Yun, Y. H.; Youngs, W. J. *Met. Based Drugs* **2008**, 384010–384016.

(34) Zhu, H.-L.; Zhang, X.-M.; Liu, X.-Y.; Wang, X.-J.; Liu, G.-F.; Usman, A.; Fun, H.-K. *Inorg. Chem. Commun.* **2003**, *6*, 1113–1116.

(35) Senko, M. *Iso.Pro 3.1*, MS/MS software, Software tools for Mass Spectrometry; http://www.ionsource.com, 2009.

(36) *APEX2, SAINT*; Bruker, AXS Inc.: Madison, WI, 2004.

(37) (a) Sheldrick, G. M. *SHELXS-97*, Program for Crystal Structure Determination; University of Göttingen: Göttingen, Germany, 1997. (b) Sheldrick, G. M. *Acta Crystallogr.* **2008**, *A64*, 112–122.

(38) Farrugia, L. J. *J. Appl. Crystallogr.* **1999**, *32*, 837–838.

(39) Spek, A. L. *Acta Crystallogr., Sect. C* **1990**, *46*, C34.

(40) Bauer, A. W.; Kirby, W. M.; Sherris, J. C.; Turck, M. *Am. J. Clin. Pathol.* **1966**, *45*, 493–49.

(41) *Performance standards for antimicrobial susceptibility testing*, 19th informational supplement M100-S19. Clinical and Laboratory Standards Institute: Wayne, PA, 2009.

(42) Bera, R.; Sahoo, B. K.; Ghosh, K. S.; Dasgupta, S. *Int. J. Biol. Macromol.* **2008**, *42*, 14–21.

(43) Lakowicz, J. R. *Principles of fluorescence spectroscopy*; Springer: New York, 2006.

(44) Mosmann, T. *J. Immunol. Methods* **1983**, *65*, 55–63.

(45) Chenskaya, T. B.; Berghahn, M.; Kunz, P. C.; Frank, W.; Kläui, W. *J. Mol. Struct.* **2007**, *829*, 135–148.

(46) (a) Shobatake, K.; Postmus, C.; Ferraro, J. R.; Nakamoto, K. *Appl. Spectrosc.* **1969**, *23*, 12–16. (b) Bradbury, J.; Forest, K. P.; Nuttall, R. H.; Sharp, S. W. A. *Spectrochim. Acta* **1967**, *23*, 2701–2704. (c) Effendy; Marchetti, F.; Pettinari, C.; Pettinari, R.; Skelton, B. W.; White, A. H. *Inorg. Chim. Acta* **2007**, *360*, 1451–1465.

(47) Geary, W. J. *Coord. Chem. Rev.* **1971**, *7*, 81–122.

(48) (a) Rosenthal, M. R. *J. Chem. Educ.* **1973**, *50*, 331–334. (b) Plakhotnyk, V. N.; Schmutzler, R.; Ernst, L.; Kovtun, Y. V.; Plakhotnyk, A. V. *J. Fluor. Chem.* **2002**, *116*, 41–44.

(49) Mohr, F.; Falvello, L. R.; Laguna, M. *Eur. J. Inorg. Chem.* **2006**, 3152–3154.

(50) Siegert, U.; Hahn, H.; Lang, H. *Inorg. Chim. Acta* **2010**, *363*, 944.

(51) (a) Capwell, R. J.; Rhee, K. H.; Seshadri, K. S. *Spectrochim. Acta A* **1968**, *24*, 955–958. (b) Miles, M. G.; Doyle, G.; Cooney, R. P.; Tobias, R. S. *Spectrochim. Acta A* **1969**, *25*, 1515–1526.

(52) Yang, L.; Powell, D. R.; Houser, R. P. *Dalton Trans* **2007**, 955–964.

(53) Reger, D. L.; Gardinier, J. R.; Smith, M. D. *Inorg. Chem.* **2004**, *43*, 3825–3832.

(54) Lorenzotti, A.; Bonati, F.; Cingolani, A.; Lobbia, G. G.; Leonesi, D.; Bovio, B. *Inorg. Chim. Acta* **1990**, *170*, 199–208.

(55) Reger, D. L.; Watson, R. P.; Gardinier, J. R.; Smith, M. D. *Inorg. Chem.* **2004**, *43*, 6609–6619.

(56) Reger, D. L.; Fole, E. A.; Smith, M. D. *Inorg. Chem.* **2010**, *49*, 234–242.

(57) Hibbs, D. E.; Hursthouse, M. B.; Malik, K. M. A.; Beckett, M. A.; Jones, P. W. *Acta Crystallogr., Sect. C* **1996**, *52* (Pt 4), 884–887.

(58) Burgoyne, A. R.; Meijboom, R.; Muller, A.; Omondi, B. B. *Acta Crystallogr., Sect. E* **2010**, *66* (Pt 5), m503–m504.

(59) Lang, H.; Leschke, M.; Rheinwald, G.; Melter, M. *Inorg. Chem. Commun.* **1998**, *1*, 254–256.

(60) Frohnapfel, D. S.; White, P. T.; Templeton, J. L.; Rüegger, H.; Pregosin, P. S. *Organometallics* **1997**, *16*, 3737–3750.

(61) (a) Reger, D. L.; Collins, J. E.; Layland, R.; Adams, R. D. *Inorg. Chem.* **1996**, *35*, 1372–1376. (b) Hunter, G.; Weakley, T. J. R.; Weissensteiner, W. *J. Chem. Soc., Dalton Trans.* **1987**, 1545–1550. (c) Miller, T. E.; Michael, D.; Mingos, P. *Transition Met. Chem.* **1995**, *20*, 533–539. (d) Otto, S.; Roodt, A. *Inorg. Chem. Commun.* **2001**, *4*, 49–52. (e) Bravo, J.; Bolãno, S.; Gonsalvi, L.; Peruzzini, M. *Coord. Chem. Rev.* **2010**, *254*, 555. (f) Phillips, A. D.; Gonsalvi, L.; Romerosa, A.; Vizza, F.; Peruzzini, M. *Coord. Chem. Rev.* **2004**, *248*, 955. (g) Pruchnik, F. P.; Smoleński, P.; Wajda-Hermanowicz, K. *J. Organomet. Chem.* **1998**, *570*, 63–69.

(62) Bi, S.; Qiao, C.; Song, D.; Tian, Y.; Gao, D.; Sun, Y.; Zhang, H. *Sens. Actuators, B* **2006**, *119*, 199–208.